Folding trajectories of human dihydrofolate reductase inside the GroEL–GroES chaperonin cavity and free in solution

Reto Horst[†], Wayne A. Fenton[†‡], S. Walter Englander[§], Kurt Wüthrich[†¶], and Arthur L. Horwich[†‡‖††]

[†]Department of Molecular Biology and [¶]The Skaggs Institute for Chemical Biology, The Scripps Research Institute, La Jolla, CA 92037; [§]Department of Biochemistry and Biophysics, University of Pennsylvania, Philadelphia, PA 19104; and [‖]Howard Hughes Medical Institute and [‡]Department of Genetics, Yale University School of Medicine, New Haven, CT 06510

Contributed by Arthur L. Horwich, October 22, 2007 (sent for review October 12, 2007)

The chaperonin GroEL binds non-native polypeptides in an open ring via hydrophobic contacts and then, after ATP and GroES binding to the same ring as polypeptide, mediates productive folding in the now hydrophilic, encapsulated *cis* chamber. The nature of the folding reaction in the *cis* cavity remains poorly understood. In particular, it is unclear whether polypeptides take the same route to the native state in this cavity as they do when folding spontaneously free in solution. Here, we have addressed this question by using NMR measurements of the time course of acquisition of amide proton exchange protection of human dihydrofolate reductase (DHFR) during folding in the presence of methotrexate and ATP either free in solution or inside the stable cavity formed between a single ring variant of GroEL, SR1, and GroES. Recovery of DHFR refolded by the SR1/GroES-mediated reaction is 2-fold higher than in the spontaneous reaction. Nevertheless, DHFR folding was found to proceed by the same trajectories inside the *cis* folding chamber and free in solution. These observations are consistent with the description of the chaperonin chamber as an ''Anfinsen cage'' where polypeptide folding is determined solely by the amino acid sequence, as it is in solution. However, if misfolding occurs in the confinement of the chaperonin cavity, the polypeptide chain cannot undergo aggregation but rather finds its way back to a productive pathway in a manner that cannot be accomplished in solution, resulting in the observed high overall recovery.

chaperonin reaction | protein folding | GroEL-mediated folding | NMR | solvent protection

Although both the polypeptide-binding and the folding-active states of the GroEL–GroES chaperonin machinery have been identified and structurally characterized (1–4), the fate of polypeptide substrates during the chaperonin reaction remains poorly understood. For example, it generally seems clear that non-native polypeptide conformational states are bound in the open ring of GroEL to hydrophobic surfaces of multiple apical domains (5–8). Yet it is uncertain whether binding in the context of a cycling reaction mediates unfolding (9, 10). There is also uncertainty concerning the mechanism of productive folding in the GroES-encapsulated *cis* cavity (11–13). Does polypeptide folding in this space take the same route to the native state as it does free in solution, or is the trajectory of folding rerouted by confinement in a hydrophilic cavity, ≈60 Å in both height and diameter, with predominantly electronegative walls (14, 15)? Does confinement itself limit the population of extended folding intermediate states that would impinge on the walls of the cavity, potentially providing an acceleration caused by entropic effects (16)?

Here, we attempt to address questions about cavity-mediated folding by using a monomeric protein, human dihydrofolate reductase (DHFR), as a substrate. After binding to GroEL upon dilution from denaturant, DHFR requires both GroES and ATP for productive folding at pH 6, thus behaving under these conditions as a so-called stringent substrate (17, 18). Yet when diluted from denaturant into the same buffer at pH 6 without GroEL, DHFR is also capable of spontaneously refolding to the native, enzymatically active state. This behavior thus allows a direct comparison of the trajectories of structure development during folding either inside the GroEL–GroES cavity or free in solution, using a strategy of amide proton–solvent deuterium exchange monitored by NMR spectroscopy. Because DHFR has a parallel β-sheet structure, the exchange studies report not only on secondary structure development but also on the acquisition of longer-range contacts that define features of tertiary structure.

Results

Rate and Extent of Recovery of Native DHFR from Folding Reactions Carried Out Either Inside the GroEL–GroES *cis* Cavity or Free in Solution. Using acquisition of DHFR enzymatic activity to monitor refolding, we compared the kinetics and extent of recovery occurring inside the GroEL–GroES *cis* cavity to that free in solution.

For assessing folding in the *cis* cavity, binary complexes of DHFR and either GroEL or a single-ring variant thereof, SR1, were prepared by diluting DHFR unfolded in 6 M GuHCl into buffer containing the respective chaperonin (similar to the NMR experiments in Fig. 1; for details see *Materials and Methods*). In such binary complexes, DHFR occupies an unfolded state as judged both by hydrogen–deuterium exchange studies (18, 19), which showed no significant exchange protection, and by direct NMR observation of the substrate, which showed no evidence of structure in its NMR-observable regions (20). In such complexes, the unfolded DHFR substrate is bound to two or more GroEL apical domains, as revealed by mutational experiments (7), but portions of the DHFR molecules may extend throughout the entire central cavity, as shown by a recent cross-linking study (8). When ATP and GroES are added to these binary complexes, bound DHFR is released into the GroES-encapsulated and now hydrophilic *cis* cavity, and productive folding then occurs. When the folding reaction is carried out at pH 6.0, there is an absolute requirement for GroES, i.e., the presence of the *cis* cavity is essential for productive folding; neither GroEL nor SR1 can refold DHFR in the absence of GroES, even after addition of ATP (18). When both GroES and ATP are added to the SR1–DHFR complex, a stable folding-active *cis* complex is

Author contributions: R.H., W.A.F., K.W., and A.L.H. designed research; R.H., W.A.F., and A.L.H. performed research; R.H., W.A.F., S.W.E., K.W., and A.L.H. analyzed data; and R.H., W.A.F., K.W., and A.L.H. wrote the paper.

The authors declare no conflict of interest.

Freely available online through the PNAS open access option.

[††]To whom correspondence should be addressed. E-mail: arthur.horwich@yale.edu.

This article contains supporting information online at www.pnas.org/cgi/content/full/0710042105/DC1.

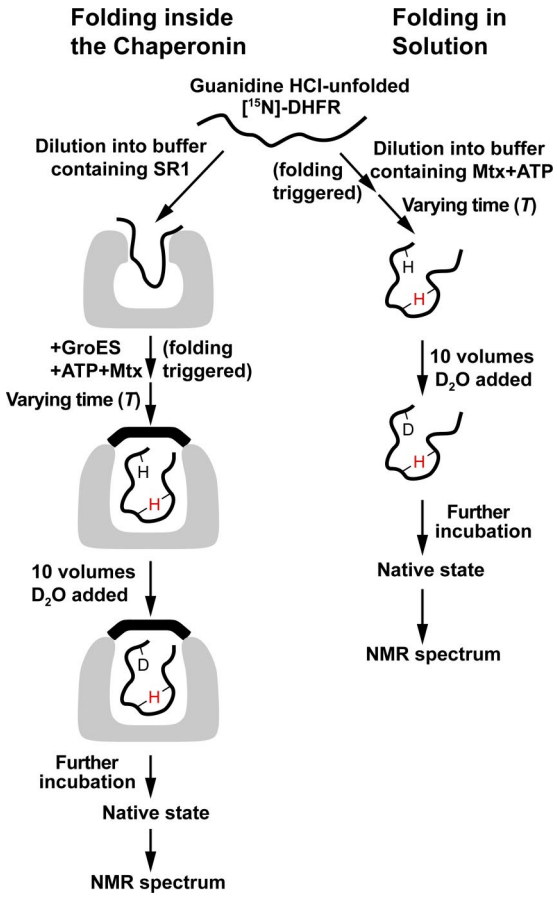

Fig. 1. Experimental set-up for analyzing DHFR refolding trajectories inside the GroEL chaperonin cavity and free in solution, using amide proton-solvent deuterium exchange monitored by NMR. *T* is the refolding time in H_2O before D_2O addition (Eq. **1**). Methotrexate was added to both experiments to stabilize the native state of DHFR. H, proton; D, deuteron.

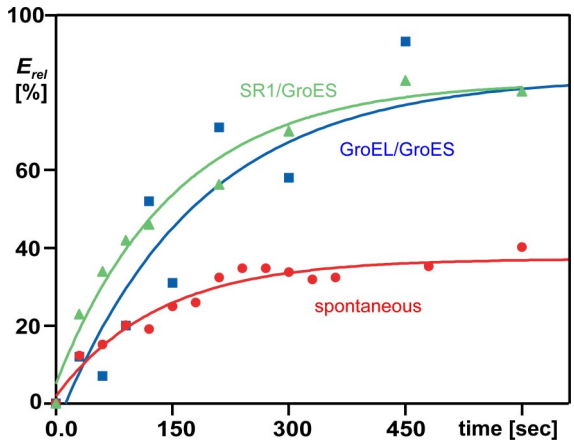

Fig. 2. Recovery of enzymatic activity of DHFR in percentage of the input native enzymatic activity, E_{rel}. For spontaneous folding, DHFR was diluted from guanidine HCl into aqueous buffer, and aliquots were taken and assayed in the presence of DHF at the time points indicated (red circles). For the chaperonin-mediated reactions, DHFR unfolded in guanidine HCl was first diluted into buffer containing either SR1 or GroEL, to form a binary complex, and the refolding reaction was then triggered by the addition of ATP and GroES, with aliquots removed and assayed for DHFR activity at the time points indicated (SR1, green triangles; GroEL, blue squares). The curves are single exponential fits to the data points.

formed (21), whereas when GroES and ATP are added to GroEL–DHFR, a cycling reaction occurs, in which folding-active *cis* ternary complexes are dissociated approximately every 10 s and then rapidly reformed (22). As shown in Fig. 2, when refolding mixtures were assayed at various times for DHFR activity, the *cis*-mediated folding reaction carried out by either GroEL/GroES or SR1/GroES was observed to proceed as a single exponential process (k = 0.0057 s^{-1} and 0.0065 s^{-1}, respectively), with a $t_{½}$ of ≈2 min and nearly full recovery of DHFR activity within 10 min (Fig. 2).

To examine refolding free in solution, guanidine HCl-unfolded DHFR was diluted into pH 6.0 buffer, and DHFR enzymatic activity was measured at various times (Fig. 2). Recovery here also exhibited single-exponential kinetics, with a similar rate constant, 0.0077 s^{-1}, but the extent of recovery amounted reproducibly to only ≈40%. In this case, a substantial fraction of the DHFR had apparently misfolded, because the protein was recovered in insoluble aggregates when the reaction mixture was centrifuged.

Amide Proton–Solvent Deuterium Exchange Monitored by NMR to Evaluate the Folding Trajectories of DHFR Inside the GroEL *cis* Cavity and Free in Solution. To further explore whether the similar rate constants observed for folding inside the chaperonin and free in solution (Fig. 2) reflect similar pathways of folding in the two locations, or whether, in contrast, the greater efficiency of folding in the *cis* cavity (Fig. 2) reflects a fundamentally different trajectory of folding, we performed amide proton–solvent deuterium exchange NMR experiments patterned after previous work by Roder and Wüthrich (23), Englander and coworkers (24), and Baldwin and coworkers (25) (Fig. 1). In particular, at various times after initiating folding, a large excess of D_2O was added and the reaction was allowed to proceed to completion, producing native [^{15}N] DHFR that was then examined by 2D [^{15}N,^{1}H] correlation spectroscopy for the level of protonation of those assigned amide protons that have protection factors in the native state on the order of 10^6 or greater (18). Quantifying the signal intensity at these "probe" positions by integrating the respective [^{15}N,^{1}H] cross-peaks provides information on the state of refolding at the time of D_2O addition. For example, if a specific proton is already hydrogen-bonded at the time of D_2O addition, then one expects that it will be protected from exchange during the completion of refolding and will therefore remain substantially protonated in the refolded native state, leading to an intense [^{15}N,^{1}H] cross-peak (Fig. 1, red H). In contrast, if a proton is unprotected at the time of D_2O addition, then one expects that it likely will be exchanged for a deuteron and have a weak [^{15}N,^{1}H] cross-peak in the refolded native form (Fig. 1, black D). Thus, by determining the degree of protection at amide proton probe positions in native DHFR in relation to various times of addition of D_2O, a trajectory of the development of hydrogen-bonded structure during the folding reaction can be read out. Because DHFR is a parallel β-sheet protein, the hydrogen bonds in the native state are formed by pairing β-strands that are, in many cases, far apart in the amino acid sequence, reflecting long-range structural organization. Thus, in the case of DHFR, the presence of hydrogen bonding also reflects the acquisition of long-range contacts along the amino acid sequence.

To analyze a stable *cis* folding reaction, avoiding any release of DHFR into solution, a folding-active SR1/GroES/[^{15}N]-DHFR ternary complex was produced by adding ATP and GroES to an SR1/[^{15}N]-DHFR binary complex (Fig. 1). In this experiment, the substrate analogue methotrexate was added to the reaction mixture to stabilize [^{15}N]-DHFR molecules reaching the native state (DHF has the same stabilizing function in the renaturation experiment of Fig. 2). At various times after

BIOCHEMISTRY

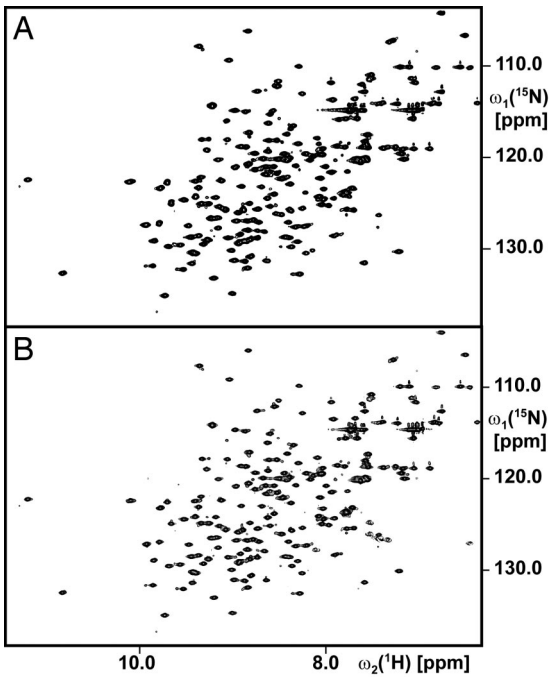

Fig. 3. 2D [^{15}N,^{1}H] HSQC NMR spectra of uniformly ^{15}N-labeled DHFR recovered after refolding in the presence of methotrexate and ATP, either mediated by SR1/GroES (*A*) or spontaneously in solution (*B*).

initiating the folding reaction, a large excess of D_2O was added, whereupon the folding reaction was allowed to continue to completion, producing native [^{15}N]-DHFR (Fig. 1). The refolded [^{15}N]-DHFR was then recovered from the SR1–GroES complex by incubation at 4°C, which releases GroES and substrates such as DHFR (26, 27), purified by ion exchange chromatography in D_2O, concentrated, and examined by NMR. The NMR experiments measured the extent of amide proton protection in 51 individually assigned probe positions, which are nonsurface residues shown previously to exhibit high levels of protection from exchange in the native state (18, 28), and thus are resistant to nonspecific exchange during subsequent steps of purification and physico-chemical measurements.

Similarly, for [^{15}N]-DHFR spontaneously refolding free in solution in the presence of methotrexate, addition of D_2O at various times, followed by completion of folding, recovery of the native [^{15}N]-DHFR, and NMR measurements, allowed observation of the hydrogen-bonded structure formed at the time of adding D_2O (Fig. 1).

NMR Experiments Reveal Similar Patterns of Acquiring Exchange Protection During Folding in the *cis* Cavity and Free in Solution. In an initial experiment we compared the spectra of DHFR refolded by SR1/GroES and free in solution in H_2O (Fig. 3). The spectra were indistinguishable and matched the previously published 2D [^{15}N,^{1}H] correlation maps of human DHFR obtained by overexpression in *Escherichia coli* and purification by methotrexate affinity chromatography (28, 29). Next, chaperone-mediated and spontaneous refolding experiments initiated in H_2O were analyzed for levels of protection from deuterium exchange at various times, T, when a large excess of D_2O was added to the folding medium (T = 15, 25, 60, and 120 s). Protection in the refolded DHFR was determined at each backbone amide proton probe position as the ratio of the integrated intensity of the corresponding cross-peak in the 2D [^{15}N,^{1}H] correlated spectrum of the refolded DHFR at the time T, I_T, and the maximal signal produced when D_2O was added after 30 min (i.e., after completion of the refolding reaction), I_{max}, yielding $A_T = I_T/I_{max}$. In addition, the zero-time peak intensity, I_0, was obtained by adding D_2O directly to the SR1–DHFR binary complex, where DHFR has been shown to be completely unprotected (18), and incubating for 15 min before starting the refolding reaction by adding ATP and GroES. A single exponential recovery curve was fitted to the variation of the ratio A_T with variable duration of folding in H_2O, T:

$$A_T = I_T/I_{max} = A_\infty - (A_\infty - A_0)e^{-\lambda_0 T}. \quad [1]$$

A_∞, A_0, and λ_0 are the fitting parameters determined by the Levenberg–Marquart nonlinear least-squares method in the CurveFit software package (www.palmer.hs.columbia.edu), analyzed with the program XMGRACE (www.plasma-gate.weizmann.ac.il). A_∞ and A_0 represent the extrapolated A_T values for infinite time and T = 0, respectively, and λ_0 represents the rate of the recovery process.

The kinetics of acquisition of protection for four representative amide proton positions is shown in Fig. 4. The acquisition of protection at the time resolution of the present NMR experiments follows single-exponential kinetics (with rate constants varying between 0.005 and 0.014 s^{-1}), although the data for several amide protons indicate that there is a preceding fast phase of folding in both the spontaneous and the SR1-mediated reactions. Correspondingly, early phases have been reported in the spontaneous reaction by tryptophan fluorescence changes (30, 31). For example, W113 in the central β-strand E exhibits an A_0 value extrapolated from the single-exponential fit (Fig. 4*B*, red and green circles) that falls well above the measured value of I_0/I_{max} (Fig. 4*B*, black diamond), indicating that extensive folding affecting this residue had occurred before the first measurement was performed at T = 15 s [see also supporting information (SI) *Text* and SI Fig. 6].

Overall, despite the 15-s "dead time" of the present NMR approach (see ref. 23), key insights into the DHFR refolding mechanism were obtained. In particular, Fig. 5 shows that the protected regions and levels of protection at both 15 s (*Left*) and 120 s (*Right*) are highly similar for spontaneous refolding (*A* and *B*) and for the SR1/GroES-mediated refolding reaction (*C* and *D*). In both reactions at 15 s, there is already a substantial level of protection in the central parallel β-sheet strands E and F (Fig. 5 *A* and *C*). In both reactions, there is then a major increase of protection in these strands during the time period from 15 to 120 sec, and additional "scorable regions" in both the central β-sheet and the flanking α-helices have become substantially protected (Fig. 5 *B* and *D*). In all of these data, there is close coincidence between the spontaneous reaction and SR1-mediated refolding.

Discussion

Same Trajectory of DHFR Folding Inside the *cis* Cavity and Free in Solution. In the presence of ATP and Mtx, the temporal development of hydrogen-exchange protection in refolding DHFR was observed to be nearly the same for folding inside the SR1/GroES *cis* cavity and free in solution. In particular, in both settings the polypeptide segments that form the central parallel β-sheet in the native state were the first to acquire significant protection (Fig. 5 *A* and *C*), followed by other regions of the sheet and the flanking α-helices (Fig. 5 *B* and *D*). This observation would indicate that long-range structure of human DHFR, involving hydrogen bond formation between nonsequential strands of the parallel β-sheet, is formed before the more local secondary structure in the flanking α-helices.

Although the observed trajectory of folding in both settings is the same, the starting points and the efficiency of the two reactions are clearly different. In solution folding, DHFR commences to fold from a urea-denatured conformation that is most

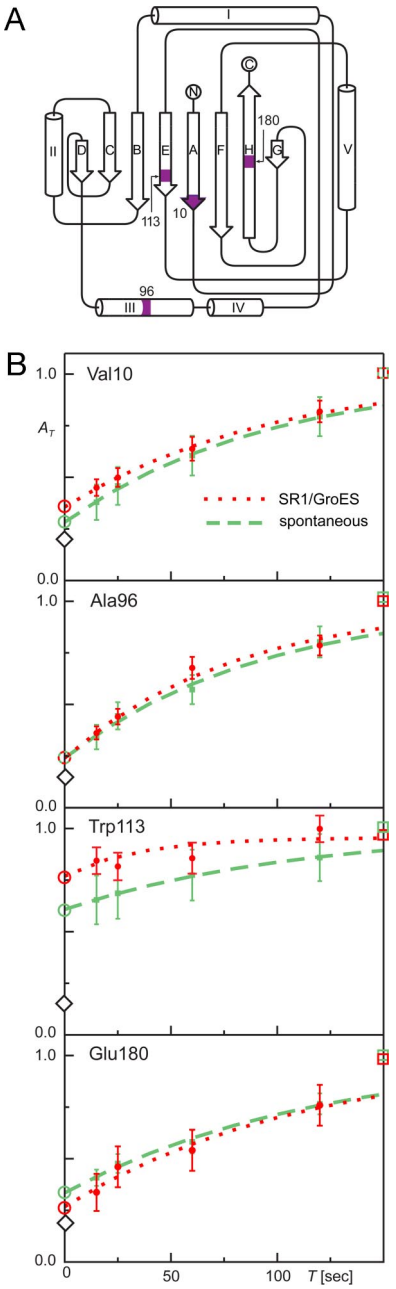

Fig. 4. DHFR refolding inside the SR1–GroES cavity (red symbols) and free in solution (green symbols) monitored by amide proton protection data measured by using the procedure of Fig. 1. (*A*) Regular secondary structures in DHFR (39) (PDB ID code 1DRF); β-strands are shown as arrows and helices are shown as cylinders. The residue positions for which data are shown in *B* are highlighted in purple and numbered. The topology plot was produced in TopDraw (40). (*B*) Plots for four amino acid residues of the relative NMR peak volumes, A_T (Eq. **1**) versus the time span after which D_2O is added to the reaction mixture, T (Fig. 1). Green and red dots represent data points for spontaneous refolding and SR1-assisted refolding, respectively. The error bars represent the precision of the peak integrals. The dotted and dashed lines are the results of nonlinear least-squares fitting of a single exponential to the experimental data, using Eq. **1**. The red and green circles on the left vertical axis are the A_0 values extrapolated from the experimental data, and the squares on the right vertical axis are the extrapolated A_∞ values. The black diamonds on the left indicate the experimental I_0/I_{max} values measured for SR1-assisted refolding.

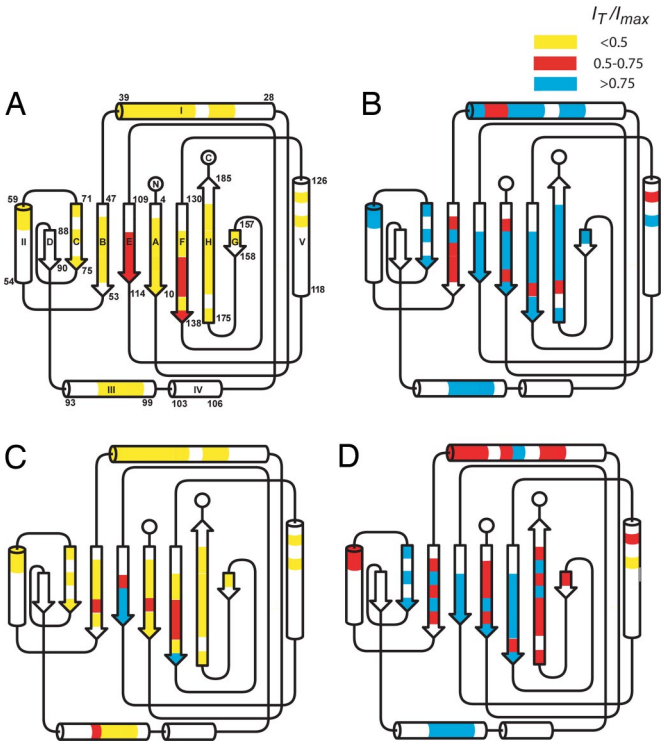

Fig. 5. Extent of proton protection measured during spontaneous refolding and SR1-mediated refolding of DHFR. (*A*) Protection after spontaneous refolding in H_2O for 15 s before the addition of D_2O. (*B*) The same as *A* after refolding in H_2O for 120 s. (*C*) SR1-assisted refolding in H_2O for 15 s before the addition of D_2O. (*D*) The same as *C* after refolding in H_2O for 120 s. Color code: yellow, $A_T < 0.5$; red, $0.5 \leq A_T \leq 0.75$; blue, $A_T > 0.75$ (see Eq. **1**).

likely a flexibly extended random coil. By contrast, in SR1-mediated folding, DHFR commences to fold from a non-native state that is bound via hydrophobic side chains to multiple apical domains of the surrounding GroEL cavity wall, a state in which the chain has been previously observed to be present in an unstructured conformation, but is likely to occupy a more collapsed state than in solution. Thus, the initial stages of folding, triggered, respectively, by dilution from denaturant or by ejection from the cavity wall into the *cis* chamber, are likely to be different. As is evidenced particularly clearly for Trp-113 (Fig. 4), a faster refolding phase than the one observed with the present NMR experiments (Fig. 1) is occurring for both SR1-mediated and solution folding and may include the aforementioned events.

A major difference between the two folding assays was observed for the efficiency of recovery, both when monitored by enzyme reactivation and during sample preparation for NMR: although there was >80% recovery of refolded DHFR in the SR1-mediated reaction, <40% recovery was measured for the spontaneous reaction (see Fig. 2). Thus, the present experiments suggest that the GroE *cis* cavity environment affects the efficiency of refolding rather than the mechanism of DHFR refolding. This indication from the experimental data can be rationalized by the assumption that DHFR may be prone to misfolding in both settings. In free solution, misfolded molecules can aggregate and are then irreversibly lost to reaching the native form. By contrast, in the hydrophilic *cis* cavity, the polypeptide folds in isolation, so that aggregation cannot occur. Misfolded states in the *cis* cavity may therefore re-enter a productive pathway, as has recently been observed in a study of *cis* folding of trypsinogen (32). Thus, given the present results, the *cis* cavity seems suitably considered to be an "Anfinsen cage," where the amino acid sequence drives polypeptide folding under confined conditions (33), and where, if misfolding occurs, the polypeptide chain does not dispose to aggregation but rather finds its way

BIOCHEMISTRY

back to a productive pathway, in a manner that cannot be accomplished in solution.

Materials and Methods

Protein Preparation. DHFR, both ^{15}N-labeled and unlabeled, was expressed in *E. coli* and purified by affinity chromatography on methotrexate-agarose (Sigma) as described (18). Unlabeled SR1 and GroES were expressed and purified as described (21).

DHFR Refolding. DHFR was unfolded by incubation in 6 M guanidinium chloride/1 mM DTT for 15 min at room temperature. It was separated from residual dihydrofolate and other small molecules by chromatography on a PD10 column (Amersham) in 6 M guanidinium chloride, 25 mM bis·Tris (pH 6.0), 20 mM KCl, and 1 mM DTT. Aliquots were quick-frozen in liquid N_2 and stored at −80°C.

For studies of spontaneous refolding, an aliquot containing 4 mg of DHFR (≈185 nmol in 0.3–0.6 ml) was thawed and rapidly diluted with vigorous stirring into 80 ml of refolding buffer A [25 mM bis·Tris (pH 6.0), 20 mM KCl, 10 mM $MgCl_2$, 1 mM DTT, 70 μM methotrexate, 2.5 mM ATP] at 15°C. After variable incubation times at 15°C, 800 ml of D_2O exchange buffer B (10 mM bis·Tris, pD* 6.0, 20 mM KCl, 5 mM $MgCl_2$, 1 mM DTT, 70 μM methotrexate, 0.5 mM ATP) at 15°C was added rapidly, and incubation at 15°C was continued for a total of 30 min. The mixture was chilled to 4°C and concentrated on an Amicon stirred cell (10-kDa cut-off membrane) to <50 ml, filtered to remove aggregates, then concentrated further to ≈0.4 ml with an Amicon Ultra 15 (10-kDa cut-off) centrifugal concentrator. The sample was diluted to 4 ml with buffer C (25 mM bis·Tris, pD* 6.0, 20 mM KCl in 90% D_2O/10% H_2O) and reconcentrated three times to remove residual methotrexate and other small molecules before the NMR measurement.

For studies of SR1-mediated refolding, a binary SR1–DHFR complex was formed by rapidly diluting a 4-mg aliquot of denatured DHFR into 75 ml of buffer D [25 mM bis·Tris (pH 6.0), 20 mM KCl, 1 mM DTT] containing ≈250 nmol (100 mg) of SR1. After a 10-min incubation at 23°C, the solution was centrifuged for 10 min at 27,000 × *g* at 23°C to remove aggregated material and then concentrated to 5 ml on a Centricon 30 (Amicon). The solution was adjusted to 10 mM $MgCl_2$ and 70 μM methotrexate, and 350 nmol (15 mg) GroES was added. This mixture was equilibrated at 15°C, and refolding was started by adding ATP to 4 mM. At variable times, the 6-ml reaction mixture was diluted with 54 ml of D_2O exchange buffer B, and the incubation was continued at 15°C for a total of 30 min. The mixture was then placed at 4°C for 30 min to release GroES and DHFR from the SR1 complex, centrifuged to remove aggregates, and chromatographed at 4°C on a POROS 50 HQ column (PerSeptive Biosystems) equilibrated in buffer C. DHFR eluted in the flow-through fractions and was concentrated on an Amicon Ultra 15 (10-kDa cut-off) centrifugal concentrator to ≈0.4 ml for the NMR measurements.

The zero time point for the SR1-assisted reaction was obtained by adding $MgCl_2$, methotrexate, and GroES to the binary SR1–DHFR complex and then diluting this mixture directly into D_2O exchange buffer B devoid of ATP. Complete amide proton exchange of the bound DHFR was achieved by incubation at 15°C for 15 min, and then ATP was added to start the refolding reaction. A 30-min incubation at 15°C was followed by 30 min at 4°C to release GroES and DHFR from SR1, and the refolded DHFR was recovered and concentrated as above.

DHFR Enzymatic Activity Assay. DHFR activity was assayed spectrophotometrically at 15°C by following the decrease in absorbance at 340 nm of a mixture containing 50 mM bis·Tris (pH 6.0), 10 mM DTT, 100 μM dihydrofolate, and 80 μM NADPH; the reaction was started by adding the enzyme. Refolding monitored by activity assay was carried out essentially as outlined above for the NMR measurements, except that it was on a smaller scale, using unlabeled DHFR and with the addition of 100 μM dihydrofolate in place of methotrexate. Aliquots of the refolding reaction were diluted directly into the assay cuvette. Recovery was calculated by comparing the initial rates to those in similar reactions with an equal amount of native DHFR.

NMR Spectroscopy. All NMR spectra were recorded on Bruker DRX-700 and AVANCE-800 spectrometers (Bruker Biospin), both equipped with triple resonance probe heads. All experiments were recorded at 25°C. The triple resonance experiments were analyzed with the CARA software package (34).

NMR Experiments Used to Monitor Refolding. A total of 256 transients were recorded for 150 complex t_1 increments of the 2D [^{15}N,^{1}H]HSQC experiment. Before Fourier transformation, a 75°-shifted sine bell apodization (35) and zero-filling was applied in both dimensions. The data were processed with the program PROSA (36) and analyzed with the program XEASY (37). Cross-peak volumes in Eq. **1** were scaled relative to the integral of a well resolved methyl resonance in 1D ^{1}H NMR spectra of human DHFR that were collected with each sample immediately before the 2D [^{15}N,^{1}H] HSQC experiment.

Sequence-Specific Backbone NMR Assignments for DHFR. The ^{1}H and ^{15}N chemical shifts of DHFR obtained by overexpression in *E. coli* and purification by methotrexate affinity chromatography (28) were used to obtain tentative assignments of the 2D [^{15}N,^{1}H] HSQC spectra of DHFR spontaneously refolded in methotrexate and DHFR recovered from the refolding reaction mediated by SR1/GroES/ATP/methotrexate. The assignments were then confirmed by using TROSY-type triple resonance experiments with uniformly [^{2}H,^{13}C,^{15}N]-labeled DHFR (38).

ACKNOWLEDGMENTS. A.H. thanks Peter Wright and Susan Marqusee for helpful discussion. K.W. is the Cecil H. and Ida M. Green Professor of Structural Biology at The Scripps Research Institute. This work was supported by grants from the National Institutes of Health and the Howard Hughes Medical Institute.

1. Thirumalai D, Lorimer GH (2001) *Annu Rev Biophys Biomol Struct* 30:245–269.
2. Hartl FU, Hayer-Hartl M (2002) *Science* 295:1852–1858.
3. Horovitz A, Willison KR (2005) *Curr Opin Struct Biol* 15:646–651.
4. Horwich AL, Farr GW, Fenton WA (2006) *Chem Rev* 106:1917–1930.
5. Braig K, Otwinowski Z, Hegde R, Boisvert DC, Joachimiak A, Horwich AL, Sigler BP (1994) *Nature* 371:578–586.
6. Fenton WA, Kashi Y, Furtak K, Horwich AL (1994) *Nature* 371:614–619.
7. Farr G, Furtak K, Rowland MC, Ranson NA, Saibil HR, Kirchhausen T, Horwich AL (2000) *Cell* 100:561–573.
8. Elad N, Farr GW, Clare DK, Orlova EV, Horwich AL, Saibil HR (2007) *Mol Cell* 26:415–426.
9. Lin Z, Rye HS (2004) *Mol Cell* 16:23–34.
10. Park ES, Fenton WA, Horwich AL (2005) *FEBS Lett* 579:1183–1186.
11. Tang YC, Chang HC, Roeben A, Wischnewski D, Wischnewski N, Kerner MJ, Hartl FU, Hayer-Hartl M (2006) *Cell* 125:903–914.
12. Farr GW, Fenton WA, Horwich AL (2007) *Proc Natl Acad Sci USA* 104:5342–5347.
13. Horwich AL, Fenton WA, Chapman E, Farr GW (2007) *Annu Rev Cell Dev Biol* 23:115–145.
14. Xu Z, Horwich AL, Sigler PB (1997) *Nature* 388:741–751.
15. Chaudhry C, Farr GW, Todd MJ, Rye HS, Brunger AT, Adams PD, Horwich AL, Sigler PB (2003) *EMBO J* 2:4877–4887.
16. Brinker A, Pfeifer G, Kerner MJ, Naylor DJ, Hartl FU, Hayer-Hartl M (2001) *Cell* 107:223–233.
17. Schmidt M, Buchner J, Todd MJ, Lorimer GH, Viitanen PV (1994) *J Biol Chem* 269:10304–10311.
18. Goldberg MS, Zhang J, Sondek S, Matthews CR, Fox RO, Horwich AL (1997) *Proc Natl Acad Sci USA* 94:1080–1085.
19. Groβ M, Robinson CV, Mayhew M, Hartl FU, Radford SE (1996) *Protein Sci* 5:2506–2513.
20. Horst R, Bertelsen EB, Fiaux J, Wider G, Horwich AL, Wüthrich K (2005) *Proc Natl Acad Sci USA* 102:12748–12753.
21. Weissman JS, Rye HS, Fenton WA, Beechem JM, Horwich AL (1996) *Cell* 84:481–490.
22. Rye HS, Roseman AM, Chen S, Furtak K, Fenton WA, Saibil HR, Horwich AL (1999) *Cell* 97:325–338.
23. Roder H, Wüthrich K (1986) *Proteins* 1:34–42.
24. Roder H, Elöve GA, Englander W (1988) *Nature* 335:700–704.
25. Hughson FM, Wright PE, Baldwin RL (1990) *Science* 249:1544–1548.
26. Todd MJ, Viitanen PV, Lorimer GH (1994) *Science* 265:659–666.
27. Rye HS, Burston SG, Fenton WA, Beechem JM, Xu Z, Sigler PB, Horwich AL (1997) *Nature* 388:792–798.
28. Stockman BJ, Nirmala NR, Wagner G, Delcamp TJ, DeYarman MT, Freisheim JH (1992) *Biochemistry* 31:218–229.
29. Prendergast NJ, Delcamp TJ, Smith PL, Freisheim JH (1988) *Biochemistry* 27:3664–3671.
30. Clark AC, Frieden C (1999) *J Mol Biol* 285:1765–1776.
31. Wallace LA, Matthews CR (2002) *J Mol Biol* 315:193–211.
32. Park ES, Fenton WA, Horwich AL (2007) *Proc Natl Acad Sci USA* 104:2145–2150.
33. Ellis RJ (2003) *Curr Biol* 13:R881–R883.
34. Keller R (2005) PhD thesis (Eidgenössiche Technische Hochschule, Zurich).
35. De Marco A, Wüthrich K (1976) *J Magn Reson* 24:201–204.
36. Güntert P, Dötsch V, Wider G, Wüthrich K (1992) *J Biomol NMR* 2:619–629.
37. Bartels C, Xia TH, Billeter M, Güntert P, Wüthrich K (1995) *J Biomol NMR* 5:327–331.
38. Salzman M, Pervushin K, Wider G, Senn H, Wüthrich K (1998) *Proc Natl Acad Sci USA* 95:13585–13590.
39. Oefner C, D'Arcy A, Winkler F (1988) *Eur J Biochem* 174:377–385.
40. Bond CS (2003) *Bioinformatics* 19:311–312.